

ICEMG 2023-Six pages

Optimization of an Axial Flux Permanent Magnet Vernier Generator for Wind Power Generation

Alireza Jaferian-Fini¹, Meysam Barghamadi², Mohammad Ardebili³

¹ Department of Electrical Engineering, K.N.Toosi University of Technology; Tehran, Iran; alireza.Jaferianfini@email.kntu.ac.ir

² Department of Electrical Engineering, K.N.Toosi University of Technology; Tehran, Iran; Meysam.Barghamadi@email.kntu.ac.ir

³ Department of Electrical Engineering, K.N.Toosi University of Technology, Tehran, Iran; ardebili@eetd.kntu.ac.ir

Abstract

Renewable energy has been the topic of much research over the years. Wind power generation, categorized as a direct drive application, requires a low-speed and high-power density generator. The permanent magnet Vernier machine is one of the flux modulation ones which can have both features simultaneously. The axial flux structure can be a better solution for this application instead of the radial counterpart with Having more power density, efficiency and compact structure. So, in this paper, a 300W axial flux permanent magnet Vernier generator (AFPMVG) TORUS type for wind power generation is investigated. with NN type magnet structure, the toroidal winding configuration is used and consequently, end winding connection is descended. The no-load phase voltage and volume of the machine is formulated. Then, the proper decision variables and primary design considerations are discussed. Using genetic algorithm (GA), the volume of the machine is optimized subjected to the constant no-load phase voltage with MATLAB software. Finally, the optimization is simulated using 3D-FEM and flux density, no-load phase voltage with harmonic orders and cogging torque are analyzed. The final design power density reached 196kW/m³. In addition, a low value in THD and cogging torque resulted, which are desired for the wind turbine.

Keywords: Axial flux permanent magnet vernier generator (AFPMVG), Genetic algorithm (GA), Power density, Finite element method (FEM).

Introduction

In recent years, direct-drive applications such as electric vehicles and wind turbines have become one of the most popular research fields [1]–[3]. Low speed and high power/torque density are needed in these applications. Mechanical gears were initially employed as a link between the machine and load or turbine as a viable option. Mechanical gears, however, have restricted reliability, high maintenance costs, and low efficiency [4].

To solve this problem, direct drive machines were proposed. These machines are coupled directly to the turbine or load, but due to the low speed of these applications, volume was increased enormously. Therefore, another type of machine was presented using a concept called magnetic gearing effect. These kinds of machines are also known as flux modulation ones. Magnetic gears, Flux switching, Flux reversal and Vernier are examples of flux modulation machines [5].

Permanent magnet vernier machine (PMVM) is one of the flux modulation types created following the evolution and integration of magnetic gears with permanent magnet machines [2]. Using the gear effect, rotor field of PMVM will rotate at speed much lower than that of armature. In this manner, the machine is capable of both working at low speed and having high power density. Many structures have been proposed for PMVM such as dual rotor, dual stator, Halbach array and so on [6]–[8].

Due to the use of integrated slot distributed winding, most of traditional PMVMs have long ending connections; as a result, volume will be increased. Toroidal winding with a high winding factor is suitable replacement for them because it reduces end winding connections and consequently, the effective diameter length. Moreover, toroidal winding can be used in machines with dual airgap and in addition to increasing the power density, for being exposed of the airgap, the cooling condition will be improved [9].

The radial flux PMVM has generally been the subject of numerous studies. However, axial flux permanent magnet vernier machines (AFPMVM) have also received interest recently. Benefiting from higher efficiency, more compact design and more significant aspect ratio, the AFPMVM is more suited for direct drive applications than the radial counterpart [10], [11]. Up to now, several AFPMVM topologies have been proposed and analyzed. In [12], the axial force between the rotor and stator of a single stator-single rotor structure is optimized and reduced. In [13], a dual stator-single rotor structure is proposed to improve the power factor. In [14], a double rotor-triple stator structure is optimized via genetic algorithm (GA). In [15]–[18], alternative topologies including dual rotor-single stator with consequent pole, triple rotor, triple stator and MAGNUS type have been examined.

Much research is conducted on the optimization of the pulsating torque and efficiency of the PM machines [19]. The PM machines have low working frequency and increase ripple of dc link capacitor in wind power generation system. Also, due to the same stator and rotor pole pairs, the rotor pole pairs can't increase significantly. Thus, in this paper, as a solution and replacement for PM generator, an AFPMVG is studied. To reduce the length of the end winding connection and boost power density, the toroidal winding will be employed in an AFPMVG with dual rotor and single stator. First, the operation principles and structure of the machine will be discussed. Second, the volume and objective function of a 300W machine will be formulated. Third, the decision variables

will be chosen and then, optimization will be performed using GA. At last, the results will be confirmed by 3D-FEM simulation.

Operation principles and structure

PMVM shares the same operating principles as permanent magnetic-geared machines [2]. The sum or difference of the number of rotor and stator pole pairs determines the number of stator teeth. As a result, the number of rotor pole pairs is more than that of armature. So, unlike

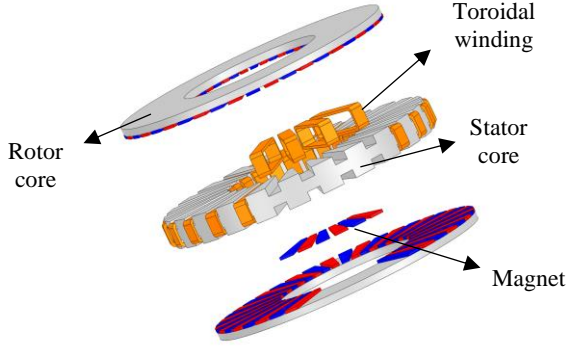


Figure 1. Exploded model of AFPMVM

permanent magnet synchronous machines, PMVMs don't adhere to the condition that the number of rotor and stator pole pairs must be equal. Due to the magnetic gearing effect, the produced MMF of rotor magnets is modulated by the stator teeth, then it is synchronized with the stator field and generates electromagnetic torque. The basic equation of PMVM is explained as (1) [1]:

$$P_r \pm P_s = Z_s \quad (1)$$

"Figure 1" shows the exploded view of AFPMVG. Overall, the structure resembles the AFPM machine, albeit with a different number of rotor poles. Magnets are designed in a trapezoidal shape to maintain constant pole arc and, as a result, a uniform flux density distribution over their surface. Utilizing the TORUS NN type machine, the toroidal winding can be used to reduce the end winding connection. It's proposed for stator design to use trapezoidal slots to mitigate cogging torque, but rectangular one is favored due to some production limits [19].

Formulating optimization problem

A. Back-EMF

The design procedure of PMVM is quite different from other types of machines because of flux modulation concept. A series flux tube between the magnet and airgap is considered. Then, the airgap flux density can be written:

$$B_g(\theta_s, r, t) = F_{pm}P(\theta_s, r) \approx F_{pm1}[\cos(P_r\theta_s - \omega t) + \frac{P_1}{2}\cos[(Z_s - P_r)\theta_s + \omega t]] + \frac{P_1}{2}\cos[(Z_s - P_r)\theta_s - \omega t] \quad (2)$$

where the P_o and P_l are calculated using conformal mapping [9]. It was supposed that the F_{pm1} , the fundamental harmonic component of magnet, is replaced the Fourier series of magnet MMF.

Using airgap flux density, the flux linkage per phase can be calculated:

$$\lambda_{ph} = k_w N_{ph} \int_{KD_o/2}^{D_o/2} \int_0^{\pi/P_s} B_g(\theta_s, r, t) r dr d\theta_s \quad (3)$$

replacing (2) in (3), λ_{ph} can be calculated as:

$$\lambda_{ph} = k_w N_{ph} (1 - k^2) \frac{D_o^2}{4P_r} F_{pm1} (P_o + \frac{6q-1}{2} P_l) \cos(\omega t) \quad (4)$$

According to the Faraday law, the back-EMF is expressed as:

$$e = -\frac{d\lambda_{ph}}{dt} = k_w N_{ph} \omega_m (1 - k^2) \frac{D_o^2}{4} F_{pm1} (P_o + \frac{6q-1}{2} P_l) \sin(\omega t) \quad (5)$$

it should be noted that it was supposed there is no saturation point in cores.

B. Sizing equations

The sizing equation of AFPMVM is the same as the AFPM machine [20]. The total diameter is given as:

$$D_{tot} = D_o + 2W_{cu} \quad (6)$$

Where for the slotted TORUS machines, the radial thickness of winding is also considered as slot depth. This thickness can be calculated as:

$$W_{cu} = \frac{D_o k - \sqrt{(D_o k)^2 - \frac{12 N_{ph} I_{rms}}{\pi k_{cu} J \alpha_s}}}{2} \quad (7)$$

The axial length of machine is given by:

$$L_{tot} = L_s + 2L_r + 2g \quad (8)$$

The stator axial length will be:

$$L_s = L_{cs} + 2L_{es} \quad (9)$$

The axial length of stator yoke can be calculated as:

$$L_{cs} = \frac{B_g \pi \alpha_p (1+k) D_o}{4 P_r B_{cs}} \quad (10)$$

The axial rotor length is expressed as:

$$L_r = L_{cr} + L_{pm} \quad (11)$$

the axial length of rotor yoke is given by:

$$L_{cr} = \frac{B_u \pi (1+k) D_o}{8 P_r B_{cr}} \quad (12)$$

For the surface permanent magnets, $B_u = B_g$. The magnet axial thickness can be written as:

$$L_{pm} = \frac{B_g \mu_r g \sigma}{B_r - B_g \sigma} \quad (13)$$

For the AFPM machines, if the number of rotor pole pairs were high, an empirical factor would be considered for axial length of rotor and stator yoke to maintain their reliability [11].

Optimization

A. Decision variables and primary design

The first step for primary design is choosing a good combination of stator and rotor pole pairs. For the direct-drive applications, the operation speed is low. For this reason, the number of rotor pole pairs should be high. Conversely, a proper combination of stator teeth number and rotor pole pair should be chosen to mitigate cogging torque at low speeds. Besides, to weaken the armature effect, a high number of stator pole pairs should be selected [6] and the most important one is that equation (1) should be satisfied. To earn all these aims, the number of stator and rotor pole pairs are chosen to be 2 and 22, respectively. The number of stator slots or teeth can be either 20 or 24, according to equation (1). Due to having low cogging torque, higher back-EMF with lower winding turns and improvement of voltage regulation, 24 is chosen [1]. "Table 1" shows the specifications of AFPMSG.

Table 1. Specifications of generator

Number	P_{out}	300(W)
Mechanical speed	ω_m	136.36(rpm)
load voltage RMS value	E_{ph}	30(V)
Number of stator pole pairs	P_r	22
Number of rotor pole pairs	P_s	2
Number of stator slots	Z_s	24

To optimize with evolutionary algorithms, the variables should be selected somehow which have the most effect on the objective function. Moreover, if there were any relationship among decision variables, it should be clearly specified for the algorithm. The determined cost function in this paper is:

$$\text{Cost function} = \text{Volume} \quad (14)$$

$$\text{Subjected to: } E_{ph} = 30 \text{ V} \quad (15)$$

B. genetic algorithm

Considering the cost function, six parameters are chosen for optimization. The outer diameter (D_o), diameter ratio (k), airgap flux density (B_g), pole arc coefficient (α_p), maximum flux density of stator (B_{cs}) and rotor (B_{cr}). Due to the nonlinearity of the equations and high number of decision variables, manual design can't reach the optimum point. So, optimization algorithms are needed to get to the minimum volume and indirectly, the maximum power density. GA is one of the optimization algorithms which originates in natural selection and

genetic manners. GA Benefits from parallel computation, solving nonlinear equations and independency of the derivations [21]. To optimize with GA, every decision variable should have an acceptable range, so that it should be neither small to limit the search zone nor large to reach a local optimization. "Table 2" shows the boundary of every variable for GA.

The range of every variable is specified around primary designed machine. Besides, some other constraints like having low cogging torque are taken into the consideration, too.

Table 2. Boundary of optimization variables

Dimension constraints	
Outer diameter (D_o)	$0.22m < D_o < 0.24m$
Diameter ratio (k)	$0.4 < k < 0.75$
Airgap flux density (B_g)	$0.4T < B_g < 1.2T$
Pole arc coefficient (α_p)	$0.65 < \alpha_p < 0.85$
Material constraints	
Stator and rotor maximum flux density	$B_{cs} B_{cr} < 1.5T$
Magnet remanence	1.21 T
Magnet permeability	1.05
Core material	M19-24G

Every variable plays the role of a gene in GA and it considers every combination of variables as a chromosome. At first, a primary population is created. Then, the reproduction process (mutation, crossover and selection) is performed and finally the superior chromosomes with the lowest cost function will be selected. This process will be continued until the stopping criteria are satisfied. The optimization is usually repeated a couple of times to make sure that it is global, not a local one.

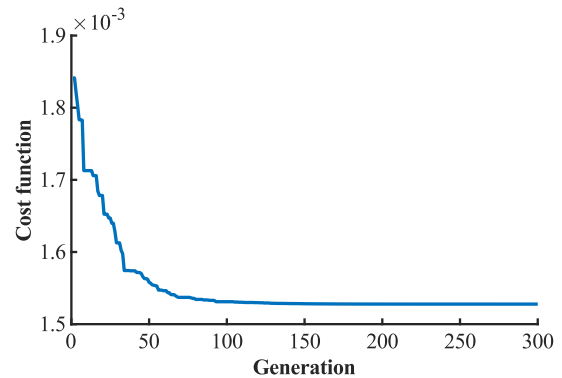


Figure 2. Convergence process of GA

"Figure 2" shows the convergence process of genetic algorithm. The population for every generation is considered to be 400. The simulation is repeated for 300 generations to reach the global optimization. After 170 generations, the GA has reached the optimum point.

The parameters of the optimized and primary machines are summarized in "Table 3".

Table 3. Final specification of AFPMVG

Parameter	Primary design	Optimized design
Outer diameter (D_o)	230 (mm)	221.2 (mm)
Diameter ratio (k)	0.6	0.51
Airgap flux density (B_g)	0.73 (T)	0.66 (T)
Pole arc (α_p)	0.83	0.72
Stator maximum flux density (B_{cs})	1 (T)	1.22 (T)
Rotor maximum flux density (B_{cr})	1.15 (T)	1.32 (T)
Slot opening(C)	0.5	0.5
Slot pitch (W_p)	23	21.8
Slot width (W_s)	11.5	10.9
Number of turns per phase (N_{ph})	200	224
Slot depth (L_{ss})	3.5(mm)	4.5(mm)
Winding radial thickness (W_{cu})	3.5 (mm)	4.5 (mm)
Magnet axial length (h_m)	3 (mm)	2.2 (mm)
Stator yoke thickness (L_{cs})	16.5 (mm)	9.4 (mm)
Rotor yoke thickness (L_{cr})	8.6 (mm)	6 (mm)
Airgap length (g)	1 (mm)	1 (mm)
Power density (ζ)	144 (kW/m ³)	196.4 (kW/m ³)

Results

The final design is processed according to GA. The 3D-FEM simulation is conducted on Ansys Electronics Desktop 2022 R1. Airgap flux density, no load voltage, harmonic orders and cogging torque are investigated.

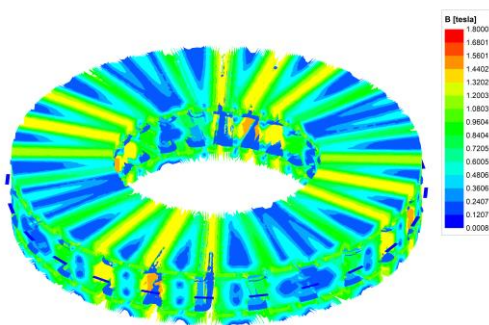
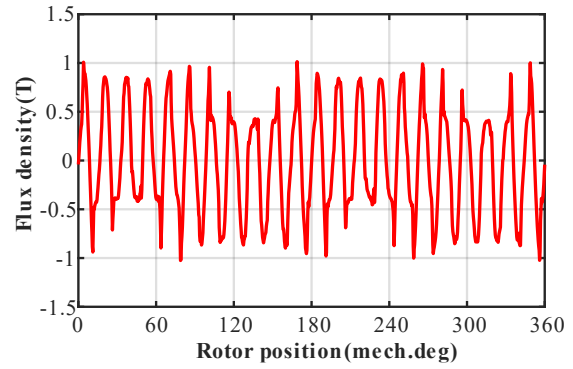
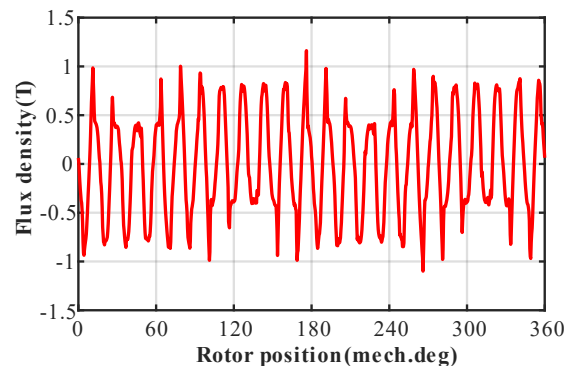


Figure 3. Flux density distribution of AFPMVG at no-load condition

"Figure 3" illustrates the flux density distribution of the optimized machine. Utilizing the TORUS NN slotted machine, the flux density closes path through the stator yoke and for the mentioned reason, the flux density is more than the other parts. The maximum flux density is 1.8T, which is less than the saturation point of the material.



(a)



(b)

Figure 4. Flux density distribution in air gaps (a) Upper air gap (b) Lower air gap

"Figure 4" presents the flux density distribution of both airgaps. The shapes are almost the same but due to the flux direction, they are inverse. The maximum flux density of airgap is 1T, which is lower than the remanence of the magnet because of high flux leakage of surface permanent magnets.

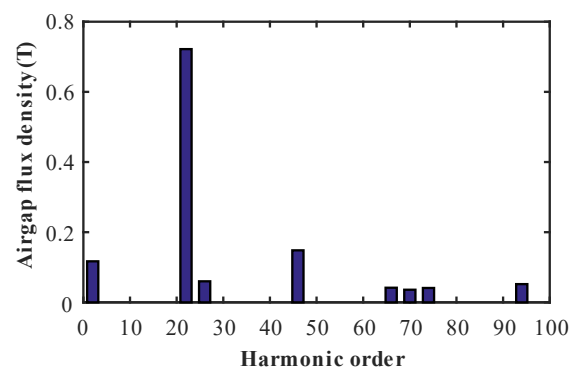


Figure 5. Harmonic order of airgap flux density

Using FFT, the harmonic spectrum of air gap flux density is plotted in "Figure 5". The prominent harmonics are 2nd, 22nd and 44th, which are the multiple of stator teeth and rotor pole pairs. The main harmonics are the 22nd and 2nd. Other harmonics with low amplitude will contribute to no-load voltage distortion, torque ripple and core loss.

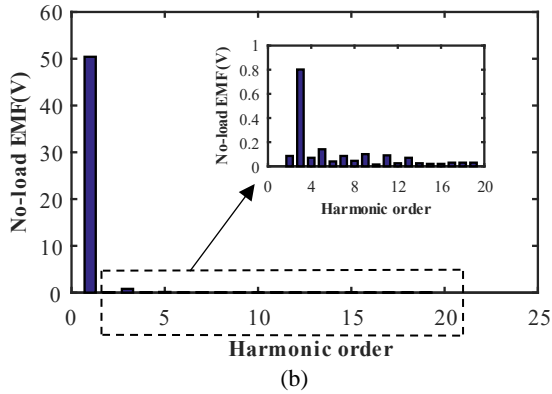
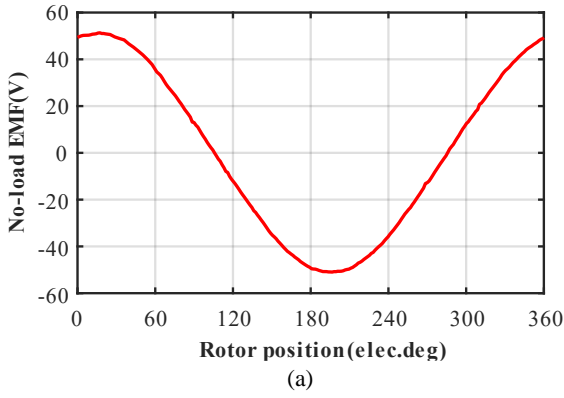


Figure 6. No-load voltage of machine (a) Voltage waveform (b) Harmonic order

"Figure 6" represents harmonic order and no-load EMF waveform. The lower total harmonic distortion (THD), the more sinusoidal waveform will be got and consequently, the stress over the dc link capacitor for wind power generation will be decreased [6]. As it can be seen in "Figure 6(b)", the amplitude of the disturbance harmonics is not comparable with the fundamental component. The calculated THD is 1.75%, which satisfies the requirements for wind power generation.

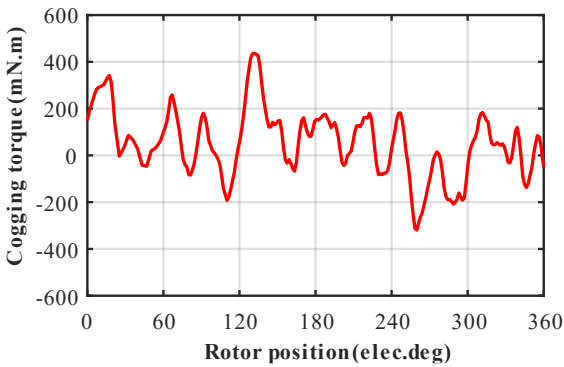


Figure 7. Cogging torque waveform

Cogging torque, already known as pulsating torque accompanied with torque ripple, is defined as result of interaction between magnets and stator teeth. Therefore, a good combination of rotor pole pairs and stator teeth will be led to the low cogging torque [19]. As shown in "Figure 7", the peak-to-peak cogging torque is 0.75N.m, which makes the machine work with low noise.

Conclusion

In this paper, an axial flux permanent magnet vernier generator with TORUS structure was analyzed. Benefiting from NN type magnet, a toroidal configuration was used to decrease the effective diameter and the volume of the machine, consequently. Using GA, the volume of the machine was optimized provided to constant no-load phase voltage. Then, the optimized generator performance was analyzed using 3D-FEM. The results of the simulation confirmed optimization. The AFPMVG showed low cogging torque and voltage THD, which is suitable for wind power generation. Besides, volume optimization was led to power density optimization, too. Despite low power, the power density reached about 196.4 kW/m³, which shows the potential of this kind of machine as a good replacement for PM machine for wind power generation.

Nomenclatures

B_{cr}	Maximum flux density of rotor core
B_{cs}	Maximum flux density of stator core
B_g	Airgap flux density
B_r	Permanent magnet remanence
B_u	Attainable flux density on surface of magnet
C	Slot opening
D_o	Outer diameter
D_{tot}	Total diameter
e	Amplitude of no-load phase voltage
E_{ph}	Phase voltage rms value
F_{pm1}	Magnet fundamental component
g	Airgap length
I_{rms}	Phase Current rms value
J	Current density
k	Diameter ratio
k_{cu}	Slot filling factor
k_w	Winding factor
L_c	Axial length of stator core
L_{cr}	Rotor yoke thickness
L_{cs}	Stator yoke thickness
L_{pm}	Magnet axial length
L_r	Axial length of rotor
L_{ss}	Slot depth
L_{tot}	Total length of the machine
N_{ph}	Number of phase winding turns
P_1	fundamental component of airgap permeance
P_o	Constant component of airgap permeance
P_{out}	Output power
P_r	Rotor pole pairs
P_s	Stator pole pairs
q	Slot per pole per phase
V	Volume
W_{cu}	Radial thickness of winding
W_p	Slot pitch
W_s	Slot width
Z_s	Stator slots number
α_p	Pole arc coefficient
α_s	Stator teeth portion to stator pole pitch portion
ζ	Power density
θ_s	Relative angle to stator axis
λ_{ph}	Flux linkage per phase
σ	Magnetic flux leakage coefficient
ω	Electrical rotor speed
ω_m	Mechanical rotor speed

References

- [1] S. P. V. Machine, A. Toba, and T. A. Lipo, "Generic Torque-Maximizing Design Methodology of Surface Permanent-Magnet Vernier Machine," *Trans. Ind. Appl.*, vol. 36, no. 6, pp. 1539–1546, 2000, doi: 10.1109/28.887204.
- [2] R. Qu, D. Li, and J. Wang, "Relationship between magnetic gears and vernier machines," *2011 Int. Conf. Electr. Mach. Syst. ICEMS 2011*, 2011, doi: 10.1109/ICEMS.2011.6073448.
- [3] D. Li, R. Qu, and T. A. Lipo, "High-power-factor vernier permanent-magnet machines," *IEEE Trans. Ind. Appl.*, vol. 50, no. 6, pp. 3664–3674, 2014, doi: 10.1109/TIA.2014.2315443.
- [4] K. Atallah, J. Wang, S. Mezani, and D. Howe, "A novel high-performance linear magnetic gear," *IEEJ Trans. Ind. Appl.*, vol. 126, no. 10, pp. 2844–2846, 2006, doi: 10.1541/ieejias.126.1352.
- [5] X. Zhu, C. H. T. Lee, C. C. Chan, L. Xu, and W. Zhao, "Overview of Flux-Modulation Machines Based on Flux-Modulation Principle: Topology, Theory, and Development Prospects," *IEEE Trans. Transp. Electr.*, vol. 6, no. 2, pp. 612–624, 2020, doi: 10.1109/TTE.2020.2981899.
- [6] J. Yu, C. Liu, and H. Zhao, "Design and Multi-Mode Operation of Double-Stator Toroidal-Winding PM Vernier Machine for Wind-Photovoltaic Hybrid Generation System," *IEEE Trans. Magn.*, vol. 55, no. 7, 2019, doi: 10.1109/TMAG.2019.2906849.
- [7] H. Gorginpour, "Dual-stator consequent-pole Vernier PM motor with improved power factor," *IET Electr. Power Appl.*, vol. 13, no. 5, pp. 652–661, 2019, doi: 10.1049/iet-epa.2018.5519.
- [8] K. Xie, D. Li, R. Qu, and Y. Gao, "A Novel Permanent Magnet Vernier Machine with Halbach Array Magnets in Stator Slot Opening," *IEEE Trans. Magn.*, vol. 53, no. 6, 2017, doi: 10.1109/TMAG.2017.2658634.
- [9] T. Zou, S. Member, D. Li, R. Qu, and S. Member, "Analysis of a Dual-Rotor, Toroidal-Winding, Axial-Flux Vernier Permanent Magnet Machine," vol. 53, no. 3, pp. 1920–1930, 2017, doi: 10.1109/ECCE.2015.7310212.
- [10] S. Kahourzade, S. Member, and A. Mahmoudi, "A Comprehensive Review of Axial-Flux Permanent-Magnet Machines," *Can. J. Electr. Comput. Eng.*, vol. 37, no. 1, pp. 19–33, 2014, doi: 10.1109/CJECE.2014.2309322.
- [11] F. Giulii Capponi, G. De Donato, and F. Caricchi, "Recent Advances in Axial-Flux Permanent-Magnet Machine Technology," *IEEE Trans. Ind. Appl.*, vol. 48, no. 6, pp. 2190–2205, 2012, doi: 10.1109/TIA.2012.2226854.
- [12] Q. Wang, F. Zhao, and K. Yang, "Analysis and Optimization of the Axial Electromagnetic Force for an Axial-Flux Permanent Magnet Vernier Machine," *IEEE Trans. Magn.*, vol. 57, no. 2, pp. 2–6, 2021, doi: 10.1109/TMAG.2020.3005216.
- [13] F. Zhao, T. A. Lipo, and B. Il Kwon, "A Novel Dual-Stator Axial-Flux Spoke-Type Permanent Magnet Vernier Machine for Direct-Drive Applications applications," *IEEE Trans. Magn.*, vol. 50, no. 11, pp. 2–5, 2014, doi: 10.1109/TMAG.2014.2329861.
- [14] K. Yang, F. Zhao, Q. Wang, and H. Lin, "Optimization Design of a Dual-Rotor Axial-Flux Permanent Magnet Vernier Machine based on Genetic Algorithm," *2019 22nd Int. Conf. Electr. Mach. Syst. ICEMS 2019*, 2019, doi: 10.1109/ICEMS.2019.8922135.
- [15] T. Zou, R. Qu, J. Li, D. Li, and L. Wu, "A consequent pole, dual rotor, axial flux vernier permanent magnet machine," *2015 10th Int. Conf. Ecol. Veh. Renew. Energies, EVER 2015*, 2015, doi: 10.1109/EVER.2015.7112967.
- [16] I. Ahmad, J. Ikram, M. Yousuf, R. Badar, S. S. H. Bukhari, and J. S. Ro, "Performance Improvement of Multi-Rotor Axial Flux Vernier Permanent Magnet Machine by Permanent Magnet Shaping," *IEEE Access*, vol. 9, pp. 143188–143197, 2021, doi: 10.1109/ACCESS.2021.3121271.
- [17] L. Wu and Z. Tian, "Analysis of a Triple-Stator Axial-Flux Spoke-Type Permanent Magnet Vernier Machine," *IEEE Trans. Ind. Appl.*, vol. 58, no. 5, pp. 6024–6034, 2022, doi: 10.1109/TIA.2022.3178686.
- [18] V. Rallabandi, P. Han, M. G. Kesgin, N. Taran, and D. M. Ionel, "Axial-field Vernier-type Flux Modulation Machines for Low-speed Direct-drive Applications," *2019 IEEE Energy Convers. Congr. Expo. ECCE 2019*, pp. 3123–3128, 2019, doi: 10.1109/ECCE.2019.8912550.
- [19] M. Aydin, Z. Q. Zhu, T. A. Lipo, and D. Howe, "Minimization of cogging torque in axial-flux permanent-magnet machines: Design concepts," *IEEE Trans. Magn.*, vol. 43, no. 9, pp. 3614–3622, 2007, doi: 10.1109/TMAG.2007.902818.
- [20] M. Aydin, S. Huang, and T. A. Lipo, "Design and 3D electromagnetic field analysis of non-slotted and slotted TORUS type axial flux surface mounted permanent magnet disc machines," *IEMDC 2001 - IEEE Int. Electr. Mach. Drives Conf.*, pp. 645–651, 2001, doi: 10.1109/IEMDC.2001.939382.
- [21] N. Taran, Mohammad Ardebili "Efficiency Optimization of an Axial Flux Permanent Magnet Synchronous Generator for Low Speed Wind," no. Icee, pp. 539–544, 2014, doi:10.1109/IranianCEE.2014.6999602.